JOURNAL OF CHEMICAL INFORMATION AND MODELING

Article

pubs.acs.org/jcim

Unlocking the Binding and Reaction Mechanism of Hydroxyurea Substrates as Biological Nitric Oxide Donors

Sai Lakshmana Vankayala, Jacqueline C. Hargis, and H. Lee Woodcock*

Department of Chemistry and Center for Molecular Diversity in Drug Design, Discovery, and Delivery, University of South Florida, Tampa, Florida 33620, United States

Supporting Information

ABSTRACT: Hydroxyurea is the only FDA approved treatment of sickle cell disease. It is believed that the primary mechanism of action is associated with the pharmacological elevation of nitric oxide in the blood; however, the exact details of this are still unclear. In the current work, we investigate the atomic level details of this process using a combination of flexible-ligand/flexible-receptor virtual screening coupled with energetic analysis that decomposes interaction energies. Utilizing these methods, we were able to elucidate the previously unknown substrate binding modes of a series of hydroxyurea analogs to hemoglobin and the concomitant structural changes of the enzyme. We identify a backbone carbonyl that forms a hydrogen bond with bound substrates. Our results are consistent with kinetic and electron paramagnetic resonance (EPR) measurements of hydroxyurea−hemoglobin reactions, and a full mechanism is proposed that offers new insights into possibly improving substrate binding and/or reactivity.

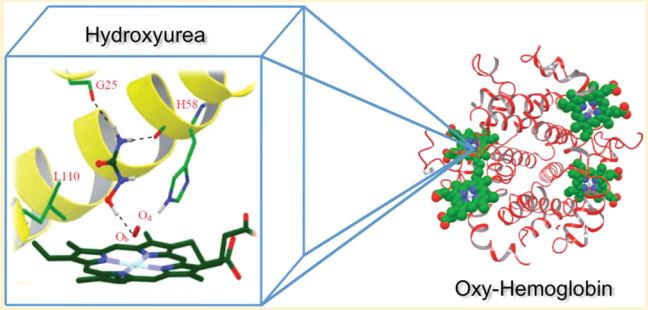

INTRODUCTION

Sickle cell disease (SCD) is an autosomal recessive disorder resulting from the mutation of the sixth amino acid in the β-globin gene changing from polar glutamic acid to nonpolar valine.[1−3] Two biomedically relevant phenotypes of hemoglobin expressed are normal adult hemoglobin (HbA) and its mutated SCD equivalent (HbS). More specifically, upon deoxygenation, mutated hemoglobin undergoes a conformational change resulting in formation of long fiberlike polymers. Polymerization of HbS inside of red blood cells distorts them into crescent shapes (i.e., sickled). Further, sickling causes the extracellular exposure of protein epitopes and glycolipids that are normally found inside the cell. Improperly exposed cellular components lead to increased adhesion of sickled red blood resulting in stroke, acute organ damage, and death.[4−6]

Two current treatment options for SCD are administration of hydroxyurea (HU) or red blood cell replacement.[7,8] Hydroxyurea, the only FDA approved treatment for SCD, involves the pharmacological elevation of nitric oxide (NO) and induction of fetal hemoglobin (HbF).[9] Watson et al. found that HbF ameliorates sickle cell severity.[10] HbF is primarily present in infants as an oxygen carrier protein during the last 7 months of gestation through the first 6 months of a newborn's life.[11] HbF is a tetramer consisting of two α and two γ globins ($\alpha_2\gamma_2$), which accounts for approximately 1% of hemoglobin in adults. HbF combines with oxygen more easily than adult hemoglobin due to the γ subunits that have more remote negative charge than its adult β counterpart.[2] In SCD patients, raising HbF levels lowers the cellular concentration of HbS and results in less polymerization hence lower incidence of sickled red blood cells. HbF also serves as a prognostic factor for sickle cell complications and pain crises.[12] Although millions of people have received this treatment, the detailed mechanism of action remains elusive.

It is thought that NO plays a key role in SCD treatment by producing smooth muscle relaxation, vasodilation, and increasing regional blood flow to help prevent cell adhesion to endothelial cells.[13] Further, NO released from the endothelium activates the NO/cGMP pathway[14] that regulates expression of the γ globin gene along with stimulation of HbF synthesis. During hydroxyurea administration, elevated levels of NO metabolites, cGMP, and HbF are observed.[15−17] Intrigued by in vivo conversion of hydroxyurea to NO along with induction of HbF, research has focused on substrate interaction with heme based proteins that catalyze redox processes. For example, oxy-hemoglobin (OxyHb), deoxy-hemoglobin (DeoxyHb), and met-hemoglobin (MetHb) have been shown to form nitrosyl-hemoglobin (HbNO), a source of NO.[2,17−19]

The structure of HbA, a tetramer assembly consisting of two α globins and two β globins, has been studied extensively.[20−26] Each of these subunits consists of a hydrophobic pocket that strongly binds the prosthetic heme group.[24] The heme group is an octahedral coordinated system with ferrous iron having four coordinate bonds to porphyrin nitrogens and a covalent bond with the proximal histidine (His87) below the plane of the

Received: January 18, 2012
Published: April 21, 2012

porphyrin ring. The sixth bond is a coordination bond with exogenous ligands such as oxygen, carbon monoxide, or nitric oxide inducing planarity of the heme. The immediate residues above the porphyrin ring plane constitute the distal pocket. Oxygen binds to HbA in a complex cooperative mechanism where the oxygen association exhibits a sigmoidal curve.[27] When OxyHb is auto-oxidized from the ferrous to ferric form it gives MetHb and superoxide[28] with the sixth coordinate position of MetHb either empty or bound by a water molecule. In contrast, DeoxyHb is generated by deoxygenation of OxyHb leaving a ferrous state iron (Figure 1).

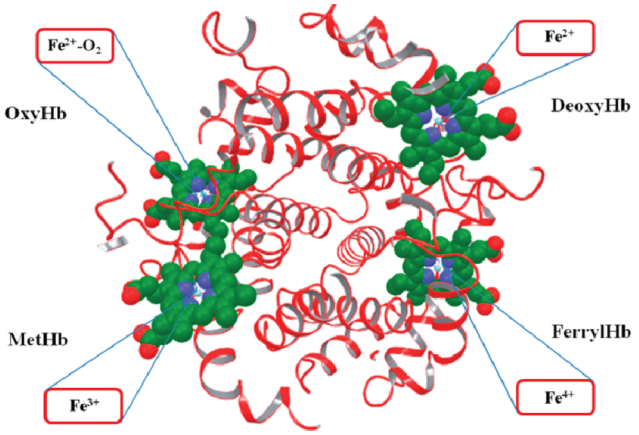

Figure 1. Generic representation of various oxidation states of iron that exist in human adult hemoglobin.[24]

In addition to its role in SCD therapy, hydroxyurea also acts as an S-phase specific chemotherapeutic agent used primarily to treat cancer. Therefore, cytotoxicity effects have been a major concern for patients undergoing treatment for SCD. This and additional properties have led to trepidation among physicians about long-term SCD treatment with hydroxyurea,[3] making the development of alternatives essential. In 2003, King and co-workers[17] designed a series of hydroxyurea analogs (HUA) depicted in Figure 2 and examined their structure activity relationship using kinetic and EPR spectroscopic techniques.

Rate constants for the reaction of OxyHb and hydroxyurea analogs forming hydroxyurea nitroxide (HU−nitroxide) radicals have been previously determined.[17,18] In that work, a reaction rate increase of 25−80 times was observed for *N*-hydroxyurea analogs compared to HU, and it was suggested these would be superior nitric oxide donors. King and co-workers[17,19,29,30] conducted several spectroscopic studies and proposed the mechanisms depicted in a series of redox reactions (Figure 3). These illustrate hydroxyurea's interaction

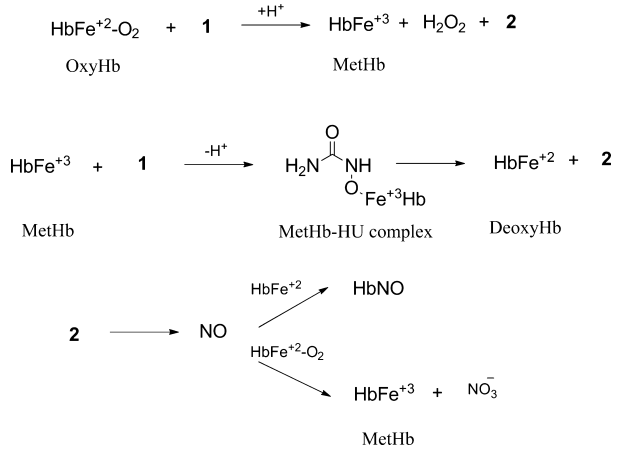

Figure 3. Generic reaction scheme presented by King and co-workers.[17]

with hemoglobin to produce NO. The in vitro reaction of all hydroxyurea analogs except **2** and **3** produced HU-nitroxide radicals with OxyHb through the abstraction of H_O by bound oxygen (O_b) to form MetHb and hydrogen peroxide. Additionally, all hydroxyurea analogs except 2, 3, and 7 were found to coordinate with MetHb to form the MetHb−HUA complex. The complexes eventually decompose to form HU−nitroxide radical (**2**) analogs and DeoxyHb. Finally, NO is

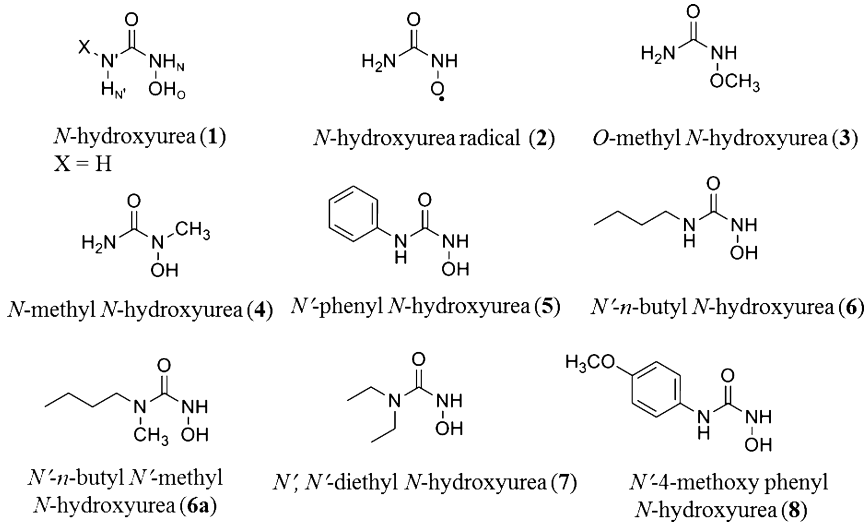

Figure 2. List of hydroxyurea analogs tested by King and co-workers from their structure−activity relationship study.[17] Defining various hydrogen atom representations: (A) hydrogen bonded to the nonhydroxyl nitrogen atom ($H_{N'}$), (B) hydrogen bonded to hydroxyl nitrogen (H_N), (C) substituent groups bonded to the nonhydroxyl nitrogen atom (X), (D) hydroxyl hydrogen (H_O). Hydroxyurea (**1**) serves as the archetype showing $H_{N'}$, H_N, H_O, and X.

dx.doi.org/10.1021/ci300035c | *J. Chem. Inf. Model.* 2012, 52, 1288−1297

formed by the decomposition of **2** and combines with DeoxyHb to form nitrosyl-hemoglobin (HbNO).[31] The study concluded that effective NO release from hydroxyurea analogs requires the formation of a low spin MetHb−HU complex. They concluded this complex could only be formed if the necessary structural features were present: an unsubstituted −NHOH group and a $H_{N'}$ atom; henceforth, analogs **2**, **3**, **4**, and **7** could not generate NO. They reasoned that the $H_{N'}$ requirement was steric in nature with the two ethyl groups bonded to N′ responsible for analog **7**'s inability to form the low spin MetHb−HUA complex.[17] However, the role of $H_{N'}$ in the complex formation was not addressed due to unavailable structural information of hemoglobin with bound substrates. Moreover, there was no discussion or comparison of the active sites of OxyHb and MetHb.

In the current work we utilize a customized induced fit docking (IFD) procedure to determine the binding modes of a series of HUA's in both OxyHb and MetHb. The IFD[32,33] protocol involves sampling dramatic side chain motions and minor backbone movement to predict OxyHb−HUA and MetHb−HUA complex structures starting from the apo conformation of OxyHb. Docking score decomposition analysis (i.e., Glide XP descriptor) is used to probe the intermolecular interactions that govern binding and stability. Sequence alignment and binding site similarity studies with α-HbA using ProBiS[34−36] and ClustalW2[37] reveal several conserved active site residues. This information, in conjunction with available structural and biochemical data,[24,30,38] is then used to propose detailed reaction mechanisms and suggest new strategies for the development of improved NO releasing substrates.

METHODS

Protein and Ligand/Substrate Preparation. X-ray crystal structure coordinates of apo OxyHb were obtained from the Protein Data Bank [PDB: 2DN1].[22] 2DN1 is a high resolution, 1.25 Å, dimer with a hydrogen bond between the distal histidine (His58) and O_d, the distal oxygen atom (i.e., farther from the central iron of the oxy-heme moiety), of both the α- and β-subunits.[39] The α-subunit was chosen because previous experimental and computational studies have shown it to have higher affinity for ligands than its β counterpart.[40−42] The impact module of the Schrödinger suite was used to predict the correct bond orders, add missing hydrogens, and remove the co-crystallized water and toluene solvent molecules. The HIE protonation state (protonated on Nε) was selected for His58 in OxyHb due to the aforementioned hydrogen bonding.[23,43,44] Subsequently, a minimization (Truncated Newton Conjugate Gradient, TNCG) employing the OPLS-2005 force field with a constant dielectric of 2 was performed freezing the oxy-heme, proximal histidine (His87),[38] and restraining (r = 2.5 Å, k = 105 kJ mol^{-1} Å^{-2}) the distance between the distal His58 hydrogen ($H_{N\varepsilon}$) and O_d.[38,42,45] Using this structure, flexible docking studies described below were carried out to generate OxyHb−HUA complexes. Subsequently, OxyHb−HUA structures were manually processed to generate MetHb−HUA starting structures for flexible docking studies, in which the bound oxygen molecule was removed, the Fe charge was converted from +2 to +3, and the Nε of His58 was deprotonated. A TNCG minimization was performed on MetHb−HUA using the same parameters applied to the OxyHb complex; however, the distance restraint between $H_{N\varepsilon}$−O_d was replaced by $H_{N'}$−O_{Gly25} (i.e., closest possible hydrogen bond). Schrödinger's LigPrep 2.3 was used to process the HUA substrates and generate energy minimized molecular structures prior to docking.

Customized Induced Fit Docking. IFD is an accurate flexible receptor/flexible ligand docking protocol which predicts binding modes by iterative combination of rigid docking (Glide)[46] with protein structure prediction (Prime).[47,48] Glide has been well validated,[49,50] while Glide/Prime has been shown to outperform other rigid and flexible receptor docking protocols.[49] This technique is ideal for X-ray structures with no bound ligand (apo structure). In such cases, amino acid side chains often protrude into the active-site restricting conformational space, resulting in the failure of rigid docking methods. The robustness and accuracy of the IFD methodology was originally validated on 21 pharmaceutically relevant protein targets by cross docking studies.[33] The IFD protocol successfully generated binding modes with ligand rmsd ≤1.8 Å for 18 of the 21 test cases. Furthermore, the 21 test cases have an average ligand rmsd of 1.4 Å when docked to the flexible receptors, while traditional rigid receptor docking yielded an average rmsd of 5.5 Å. Alternative approaches for incorporating flexible receptors into ligand docking protocols exist; however, common procedures like explicit solvent MD simulations have experienced limited success in predicting protein−ligand complexes.[33] This limitation is a result of several factors, with two aspects being particularly problematic. The first is the necessity for accurate small molecule force fields.[50−52] This is an active area of research, but presently there is no comprehensive solution. A second problem exists if significant active site reorganization is required for ligand binding. In this case, extensive simulations (up to microseconds) may be required to cross the high energy barriers of side chain and/or backbone rearrangement. Kolossavry et al.[53] encountered this difficulty when predicting 9-deaza-9-benzylguanine binding modes to purine nucleoside phosphorylase (PNP). In contrast, IFD incorporates both side-chain and backbone flexibility in a more computationally efficient manner. This has been extremely useful for a wide variety of computational biology studies.[54−59] For example, Celik et al.[55] showed that IFD was able to prospectively predict the binding mode of ligand neurotransmitter serotonin (5-HT) to the human serotonin transporter (hSERT). Additionally, Barreca et al.[60] predicted the binding mode and mechanism of action of integrase strand transfer inhibitors in the target HIV-1 integrase.

A customized IFD protocol was used to induce protein flexibility into the apo structure of OxyHb with the same protocol used for MetHb−HUA complexes. The following steps were undertaken with an in-house python script developed to automate the process (Figure 4).

(1) Mutated flexible active site residues: The first step of this process involves mutating all residues within 7 Å of the oxygen of oxy-heme to alanine. The distal and proximal histidines, His58 and His87, respectively, were excluded from this process, as they were deemed essential to the structure.

(2) Initial Glide docking: Hydroxyurea analogs were docked into the OxyHb and MetHb active sites, using Glide standard precision (Glide SP). Dockings were carried out with vdW scaling of 0.5 for the ligand and 0.7 for both receptors, while H_O was required to be within 2.3 Å of the bound oxygen (O_b) in OxyHb[17] and 2.5 Å from the

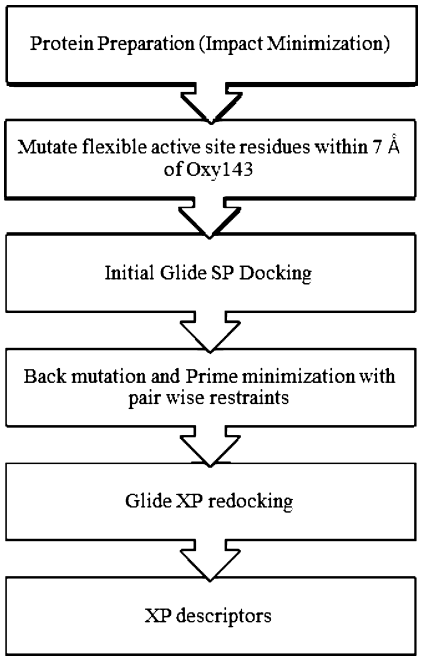

Figure 4. Flowchart of IFD protocol followed to predict the binding modes of hydroxyurea analogs in OxyHb and MetHb.

deprotonated Nε (His58) in MetHb. We requested 100 poses of partially optimized receptor−substrate complexes to allow for extensive conformational examination.

(3) Prime refinement: Each Glide SP receptor-substrate output pose was refined by prime, which performs side chain prediction by back mutating the alanine residues to their initial amino acid. Back mutation was followed by minimization of the entire receptor-substrate complex. This was done while retaining the original frozen atoms and restraints (k = 200 kJ mol^{-1} Å^{-2}) from Glide SP. Again, in MetHb the $H_{N\varepsilon}$−O_d distance restraint was replaced by $H_{N'}$−O_{Gly25} with the force constant for this interaction reduced to 25 kJ mol^{-1} Å^{-2}. A TNCG minimization with full vdW radii for the receptor−substrate complex was again performed using the OPLS 2005 all-atom force field with surface generalized Born solvation energies. Following all minimizations, structures within a 40 kcal mol^{-1} energy window were retained for redocking (~50−100 structures).

(4) IFD-XP redocking: Glide extra precision (Glide XP) redocking was performed with a single positional restraint for both OxyHb and MetHb. The restraints required H_O atoms to be within 2.5 Å of the oxygen O_b for OxyHb and His58 Nε for MetHb. XP descriptor information for the best redocked (i.e., scored) ligand/substrates poses was analyzed.

RESULTS

Docking results of hydroxyurea analogs into OxyHb[16,17,30,38] were obtained to gain insight into the binding modes and redox reactions that produce NO in SCD treatment. The binding modes were analyzed using the Glide XP scoring function, which is broken down into individual interaction energies. These descriptors are viewable with the "XP Visualizer" program in Maestro. The score includes favorable energy terms such as the chemscore−lipophilic pair term (Lipophilic EvdW), hydrophobic enclosure (PhobEn), hydrophobically packed hydrogen bonding (PhobEn HB), chemscore hydrogen-bond interactions (HBond), electrostatic interaction (Electro), and low molecular weight (Low MW). The cumulative penalty term (Penalty) includes intraligand contacts, polar atom burial, amide torsion, and desolvation. The best-docked pose for all hydroxyurea substrates in OxyHb was retained for the XP descriptor analysis (Table 1). From the IFD results, Leu29, Phe33, Phe43, Phe46, Leu48, Val62, and Ala63 positions underwent substantial change where the rmsd was 0.50−4.36 Å when compared to initial positions (Table S1 in the Supporting Information). All rmsd values were calculated with CHARMM[61−63] as it was necessary to account for atom reordering that occurred during Prime's back mutation procedure.

The corresponding substrate representative binding modes are shown in Figure 5. All substrates except **7** (Figure 5b) show H_O hydrogen bonded to the bound oxygen atom (O_b) and their $H_{N'}$ hydrogen bonded to the O_{Gly25}. **1** and **4** have similar binding modes. Only **7** has a unique binding mode, whereas **5**, **6**, and **8** have congruent binding modes.

IFD was also performed for MetHb with the restraints described in the Methods section. The XP descriptor analysis results are presented in Table 2, and Figure 6 illustrates predicted binding poses of **1**, **7**, and **8**. IFD caused the following residues, Leu29, Phe33, Phe43, Phe46, Leu48, Val62, and Leu105, to undergo substantial change: rmsd 0.60−3.92 Å compared to their respective OxyHb complexes (Table S2 in the Supporting Information). Our results show that **7** has the smallest hydrogen bonding contribution in MetHb due to the lack of a hydrogen bond between $H_{N'}$ and O_{Gly25}. Also, **5** and **8** have similar binding modes with significant hydrophobic stabilization.

DISCUSSION

The current work seeks molecular level insight into the binding modes and reactions for a series of hydroxyurea analogs in OxyHb and MetHb. Until now, details of these processes have remained elusive, largely due to the lack of co-crystallized structural information. Current results combined with previous structural[20,26,30] and biochemical information[16,17,30] allow for

Table 1. XP Descriptor Analysis Derived from IFD-XP Redocking of Hydroxyurea Analogs into OxyHb, Compared with the Reported Experimental Rate Constants

name	XP score	Lipophilic EvdW	PhobEn	Phob En HB	HBond	Electro	Low MW	Penality	rate constant k_1(min^{-1}) with OxyHb[17]
1	−4.59	−0.45	0.00	0.00	−2.77	−0.92	−0.50	0.05	$7.54 \times 10^{-4} \pm 2.16 \times 10^{-5}$
4	−4.42	−0.93	0.00	0.00	−2.50	−0.49	−0.50	0.01	$3.93 \times 10^{-2} \pm 1.68 \times 10^{-3}$
5	−6.48	−3.10	−0.68	0.00	−2.08	−0.43	−0.50	0.31	$6.24 \times 10^{-2} \pm 6.18 \times 10^{-3}$
6	−5.36	−2.33	−0.25	0.00	−1.89	−0.40	−0.50	0.01	$8.56 \times 10^{-3} \pm 1.87 \times 10^{-4}$
7	−4.57	−2.27	0.00	0.00	−1.72	−0.09	−0.50	0.01	$2.26 \times 10^{-3} \pm 8.16 \times 10^{-5}$
8	−7.35	−3.54	0.00	−1.50	−1.63	−0.46	−0.50	0.27	$1.94 \times 10^{-3} \pm 5.50 \times 10^{-4}$

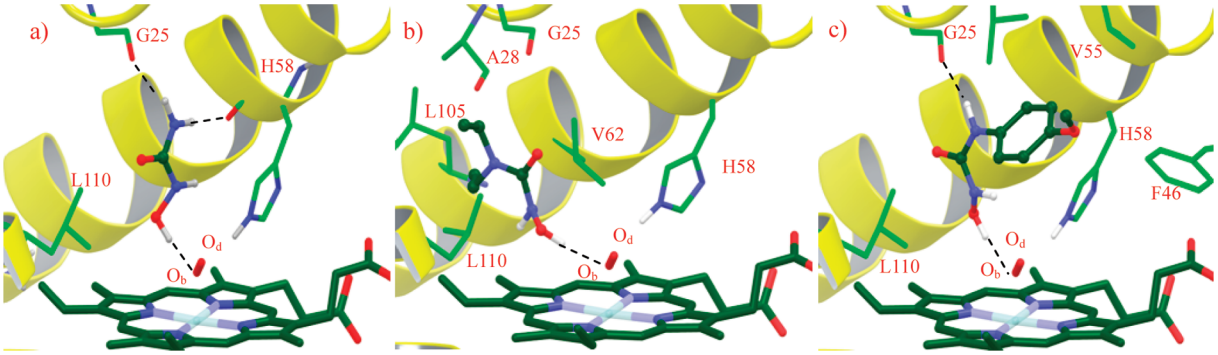

Figure 5. Predicted binding modes of the hydroxyurea analogs, **1**, **7**, and **8** in OxyHb. Carbons of heme and ligands are colored green; oxygen, red; nitrogen, blue; sulfur, yellow; hydrogen, gray; and iron, light blue. Hydrogen-bonding interactions are shown as black dashed lines, and the active site loop is highlighted as a yellow ribbon.

Table 2. XP Descriptor Analysis of All Hydroxyurea Analogs Obtained from IFD-XP Redocking in MetHb

name	XP score	Lipophilic EvdW	PhobEn	PhobEn HB	HBond	Electro	Low MW	Penality
1	−3.27	−0.56	0.00	0.00	−1.76	−0.56	−0.50	0.10
4	−3.31	−0.95	0.00	0.00	−1.62	−0.30	−0.50	0.07
5	−7.80	−2.76	−0.78	−1.50	−1.62	−0.78	−0.50	0.16
6	−3.93	−2.16	0.00	0.00	−1.61	−0.38	−0.50	0.72
7	−4.13	−2.14	0.00	0.00	−1.33	−0.33	−0.50	0.17
8	−6.03	−3.42	0.00	−1.50	−1.35	−0.24	−0.50	0.99

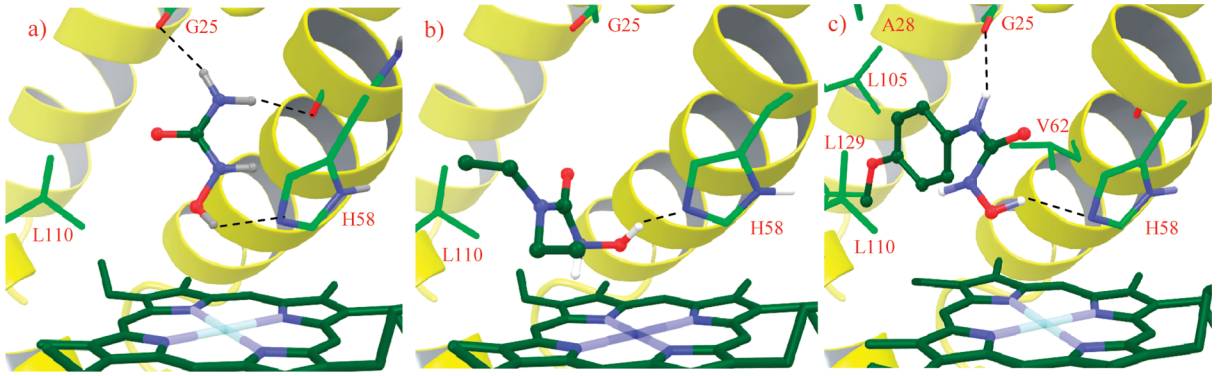

Figure 6. IFD structures for predicted binding modes of the hydroxyurea analogs **1**, **7**, and **8** in MetHb are depicted in parts a, b, and c, respectively.

the first prediction of HU (and analogs) binding and subsequent reaction mechanism.

The putative narrow OxyHb substrate binding site consists of several hydrophobic residues, oxy-heme, and His58; an imidazole functional group that acts as a ligand gate for entry into the OxyHb active-site.[43] His58 also acts as a proton donor in the proposed mechanism (Figure 7a). In this reaction, the nature of Fe−O_2 bonding exists in accordance with the Weiss bonding model,[24,38,45] in which a single electron transfer from Heme−Fe^{II} to O_b leads to a Heme−Fe^{III}−O_2^- complex.[24,64] Soon after the radical localizes on the bound oxygen, we hypothesize it will be transferred to the hydroxyurea substrates by abstracting H_O, leaving **2** (Figure 7a). Subsequently, a negative charge generated on O_d will abstract hydrogen from His58 forming H_2O_2. Since the first step involves H_O abstraction in all the hydroxyurea substrates, we performed IFD studies with an explicit positional restraint enforcing the H_O to be within 2.5 Å of the O_b. The OxyHb studies revealed that all analogs fit well in the active site that is surrounded by various hydrophobic residues. Leu29, Phe33, and Val62 experienced the greatest active site conformational rearrangement due to accommodation of substrates during the IFD procedure (Supporting Information Table S1).

Figure 5 illustrates that all hydroxyurea analogs preferentially form a hydrogen bond to O_{Gly25} except for **7**, due to the absence of $H_{N'}$. Hence, the total XP hydrogen bonding score for **7** (PhobEn Hb + Hbond) derived from IFD has the smallest contribution to the total Glide score. The hydrophobic substrate groups, phenyl, *n*-butyl, and methoxyphenyl bonded to N′ of **5**, **6**, and **8**, respectively, occupy a well-defined hydrophobic cavity in OxyHb created by Leu29, Met32, Phe43, Phe46, Leu48, Val55, and His58. These additional hydrophobic interactions (Lipophilic EvdW + PhobEn) increased stabilization by 2.5−3.8 kcal/mol. The enhanced hydrophobic contribution of **5** and **8** compared to **6** can be attributed to partial π-stacking between the side chain of His58 and their corresponding phenyl and methoxyphenyl substituents; clearly seen in Figure 8. Substrate **8** has even better binding affinity to OxyHb than **5** due to the additional hydrophobic contribution from the methoxy group with Leu29, Phe33, Phe46, and Val55 (Figure 5). The tighter binding may be correlated to **8** having a

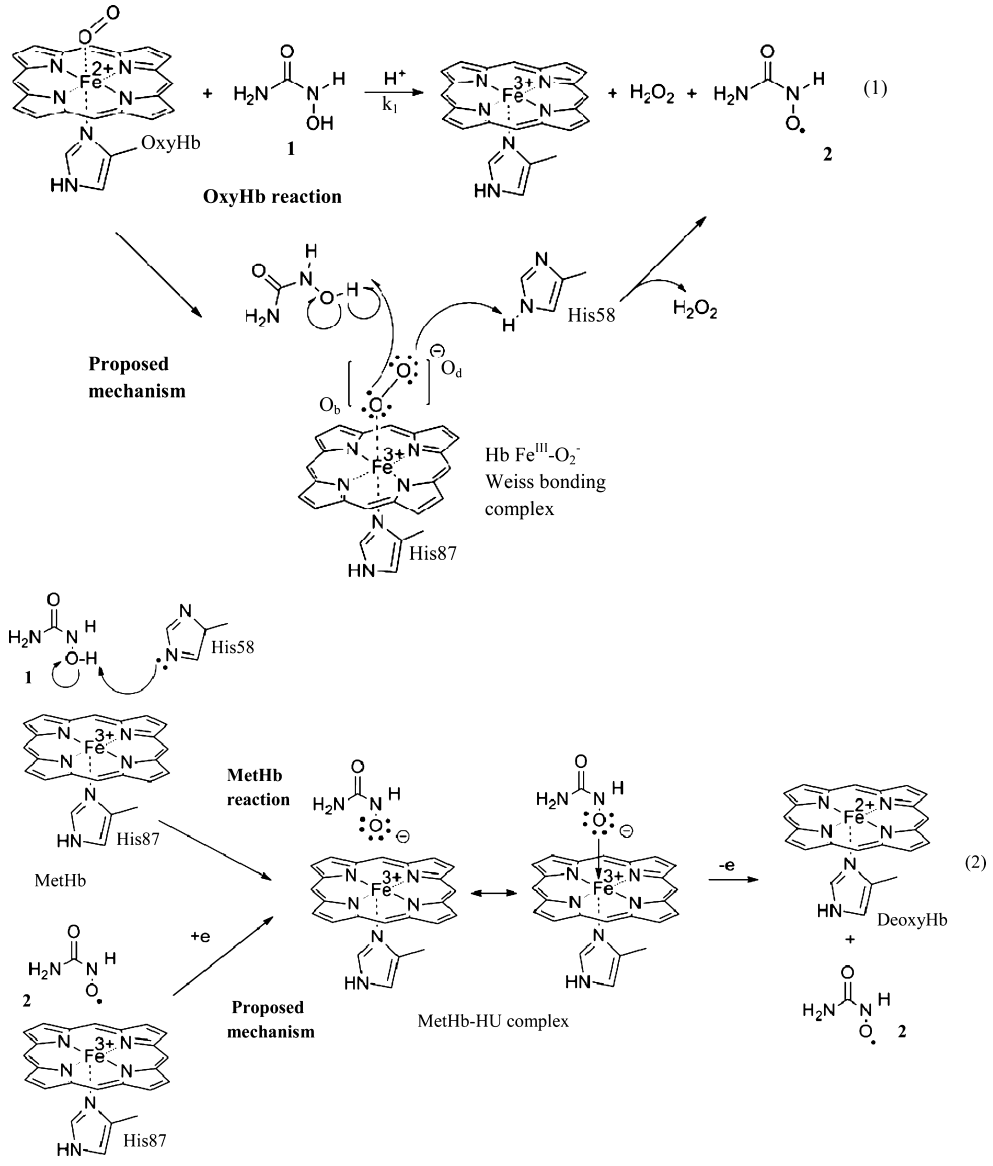

Figure 7. Proposed mechanism of action between hydroxyurea analogs and adult hemoglobin. (a) Reaction scheme 1 demonstrates interaction of **1** with OxyHb to give hydroxyurea nitroxide radical (**2**). (b) Reaction scheme 2 shows the possible mechanistic interactions between **1**/**2** and MetHb to produce DeoxyHb and **2**. Here, :→ is the classical dative bond representation.

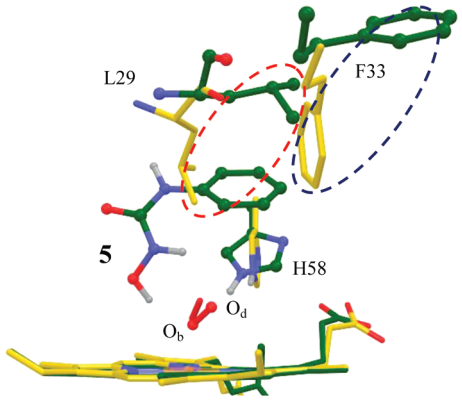

Figure 8. Comparison of the induced fit conformation of OxyHb with **5** (in dark green) and apo structure of OxyHb (in yellow). All hydroxyurea analogs in general induce receptor flexibility by generating a Leu29 flip, which further moves away Phe33.

smaller rate constant than **5** when reacting with OxyHb (Table 1).[17]

Custom IFD was undertaken based on the proposed mechanism in Figure 7b. Results showed that **7** has less hydrogen bonding stabilization in MetHb compared to OxyHb. This stabilization is hypothesized to be necessary to retain the substrate radicals/anions in MetHb (Figure 7b) and suggest an explanation as to why **7** does not form a low-spin MetHb–HUA complex,[17] a prerequisite in the formation of HbNO. A closer inspection of docking scores and XP descriptors reveals only modest differences in stabilizations and penalties comparing 7-OxyHb and 7-MetHb. This suggests that steric clashes, which have been previously hypothesized as the cause of **7** not producing NO are not likely responsible. Again, this supports our hypothesis that the lack of hydrogen bonding to O_{Gly25} is the more likely explanation.

To further support our hypothesis, that steric repulsion is not the cause of **7**'s lack of reaction, we have modified analog **6** when bound to MetHb by replacing the hydrogen bound to N′

dx.doi.org/10.1021/ci300035c | J. Chem. Inf. Model. 2012, 52, 1288–1297

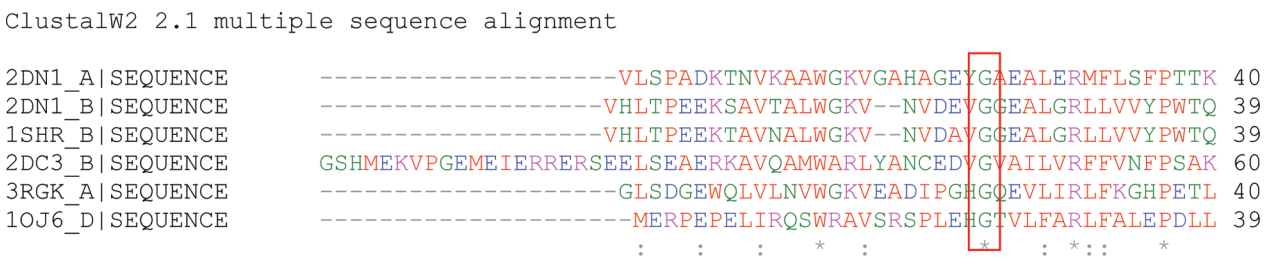

Figure 9. Mutiple sequence alignment studies of human globin chains includes α-Hb, δ-Hb, β-Hb, cytoglobin, myoglobin, and human neuroglobin using ClustalW2 in which 2DN1-A was used as the query protein. Legends given below the sequences represent residues that are identical ("*"), observed conserved substitutions (":"), and observed semiconserved substitutions ("."). The amino acid residues are colored according to their physiochemical properties in which red implies small hydrophobic (AFILMPVWY); blue implies acidic (DE); purple implies basic (HKR); and green implies with hydroxyls and amines and basic too (CGHNQSTY).

with a methyl group constructing **6a**. This complex "should" represent a more sterically hindered environment. The protein complex, **6a**, was minimized until the rmsd reached a maximum cutoff of 0.30 Å from the explicit coordinate geometry of **6** using the TNCG algorithm and later the ligand was scored in place by the Glide XP docking algorithm. XP descriptors were obtained to compare **6** and **6a** (Supporting Information Table S3). As anticipated, the ΔH bond difference was 0.92 kcal mol^{-1}, indicating a significant loss of hydrogen bonding stability for **6a**. The methyl bonded to the N′ atom improved the lipophilic vdW contribution by 0.1 kcal/mol and surprisingly reduced the penalties from 0.72 to 0.16 kcal mol^{-1}. These results again demonstrate the importance of the $H_{N'}$ atom for hydrogen bonding and shows that adequate space is available to accommodate additional substituents on the N′ atom.

The XP descriptor analysis explains the observed difference in the binding modes of **5** and **8** in OxyHb and MetHb (Figures 5 and 6, respectively). The different conformation of **5** and **8** in MetHb is attributed to the loss of a hydrogen bond interaction with O_b that is required to stabilize the protein−substrate complex. Therefore hydrophobic substrate groups, phenyl and methoxy phenyl on the N′ atom of **5** and **8**, respectively, occupy a different well-defined hydrophobic cavity created by Gly25, Ala28, Val62, Leu101, Ser102, Leu105, and Leu129 in MetHb (Figure 6c). We also observe contrary binding affinities in the case of MetHb, as shown by **5** having a lower docking score than **8** (Table 2). We attribute this to unfavorable steric interactions by the methoxy subgroup within the hydrophobic cavity that lead to high penalties. Hence, we propose hydroxyurea substrate design for effective NO release should involve optimizing the interactions between hydrophobic substituent (X) and hydrophobic residues in the active site of OxyHb and MetHb while ensuring that there is a hydrogen bond between the $H_{N'}$ atom and O_{Gly25}.

To gain further insight into the importance of Gly25 and the aforementioned hydrophobic residues, we examined active site conservation using a protein binding site detection tool (ProBiS)[34−36] along with ClustalW2.[37] ProBiS uses a database of 29 412 nonredundant PDBs to represent structural diversity. This group is searched using a novel algorithm based on the clique approach[65] that effectively identifies binding site topologies with similar geometric and physicochemical properties to the query protein. Using the adult hemoglobin HbA [PDB ID: 2DN1-A chain] as the query protein, ProBiS yielded 302 protein structures with similar binding site topologies. The proteins with *Z*-scores (statistical measure of protein similarity) > 2 were analyzed with additional similarity calculated using local structural alignment. The local structural similarity *Z*-scores along with the Pfam entities are depicted in the SI (Figure S2).

ProBiS's structure based sequence alignment results showed the most conserved active site residues to be Phe43, His58, Val62, Leu83, His87, Phe98, Leu100, and Leu101 and the most conserved substituted residues to be Gly25, Leu29, and Phe46. Conservation is present across all 302 nonredundant structures with human globin proteins such as cytoglobin, myoglobin, β-HbA, δ-HbA, and neuroglobin having similar binding sites to α-HbA and high sequence identity. Sequence alignment using these six proteins was subsequently carried out with ClustalW2. Results revealed Gly25, Phe43, His58, Val62, and His87 to be the most conserved residues with Phe46, Leu83, Phe98, Leu100, and Leu101 being the most conserved substituted residues (Figure 9 and Supporting Information Figure S3). The identification of conserved Gly25 and important hydrophobic residues provides further evidence supporting our above recommendations.

As previously mentioned, King and co-workers observed a large rate increase for **5** and **8** as compared to **1**. They attributed this effect to the presence of aromatic substituents and their ability to stabilize the initially formed nitroxide radical (similar to **2**).[17] There is some controversy surrounding this prediction as Rohrman and Mazziotti computationally examined the radical stabilization of King's HU derivatives.[18] They predicted the enhanced rate of **5** was most likely due to transition state stabilization as it had a very small radical stabilization, in apparent contrast with King's hypothesis. Rohrman et al. also suggested that longer alkyl chains at the **X** position should improve substrates; however, they were unable to confirm these were sterically allowed in the OxyHb active site. From the large rmsd's (0.5−4.36 Å) induced by substrate docking in OxyHb, we conclude the hydrophobic pocket is a possible source of the previously hypothesized transition state stabilization. Additionally, the newly predicted H_O-O_{Gly} hydrogen bond helps to further clarify the observed reactivity and positions itself as another possible source of transition state stabilization.

Although the exact mechanism of radical production from hydroxyurea analogs with MetHb is unclear, our docking studies give insight into likely reactions. Examining the importance of $H_{N'}$ binding contributions to the total binding affinity lead us to explore the low-spin MetHb−HUA complex formation. This yields three possible hypotheses A, B, and C for MetHb reaction scheme 2. Hypothesis A entails a new substrate molecule entering MetHb by replacing the existing substrate radical from reaction 7a as proposed by King and co-workers.[17] However, it is unclear as to what happens to the radical once it leaves the active site as it will most likely get quenched and not

be retained for the third reaction (Figure 3). In hypothesis B, the substrate radical will be retained in the active site through the stable hydrogen bonding interaction between $H_{N'}$ and O_{Gly25}. Furthermore, adequate data in the literature[66−68] supports the plausibility of hypothesis B, in which various electron transfer reactions occur commonly either in solvent media or intra- or intertetramer subunits of hemoglobin. The complex array of hemoglobin electron transfer mechanisms indicates that an electron can easily be transferred to the hydroxyurea nitroxide radical to form the hydroxyurea nitroxide anion. The anion would then coordinate to the ferric iron of MetHb to form a low-spin MetHb−HUA complex. Hypothesis C is similar in mechanistic detail to hypothesis A, except that the hydroxyurea analog substrate is reformed from the interaction of the substrate radical and a hydrogen radical abstracted from an active site water molecule. Because the active site is at the surface of hemoglobin subunits, water should be available to facilitate this mechanism. After scrutinizing hypotheses A, B, and C, it seems likely that either the hydroxyurea anion substrate or the hydroxyurea substrate radical will be retained in the active site by the hydrogen bond to O_{Gly25} and react to form the low spin MetHb−HUA complex.

CONCLUSION

Sickle cell anemia is an inherited disease that causes sickling of red blood cells. There is a growing need for drugs that can effectively release NO to ease the intense pain and also elevate HbF levels that possess better oxygen affinity than HbA. Unfortunately, the discovery of novel drug substrates that produce effective NO release has been hindered by the lack of structural information focusing on the interaction between Hb and hydroxyurea, the only FDA approved SCD treatment. In the current work, we employed an effective docking protocol to obtain the first bioactive 3D models of OxyHb and MetHb with a congeneric series of hydroxyurea analogs. Furthermore, we proposed reaction mechanisms (Figure 7a and b) based on combined information obtained via binding modes and previous biochemical data. IFD results and the proposed mechanisms offer new insights into key intermolecular interactions that may be exploited during rational substrate/drug design.

The current work elucidates the importance of the $H_{N'}$ atom and its contribution as a vital stabilizing interaction. This sheds new light onto the previously observed HUA $H_{N'}$ requirement.[17] XP descriptor analysis also yields insight into key structural requirements for small molecules interacting with OxyHb and MetHb. Substrates having aromatic functional groups are shown to have better binding affinity than other hydroxyurea analogs in Hb due to their favorable van der Waals, π-stacking and hydrophobically packed hydrogen bonding energy[46] contributions. Our observations show that to achieve better substrate design for effective NO release, it is important to consider the exploitation of this key $H_{N'}$ bonding interaction with O_{Gly25}, along with maximizing the hydrophobic interactions within the deep hydrophobic pocket of hemoglobin.

Furthermore, from observed binding site similarities and high percent sequence identities to α-HbA, we hypothesize that hydroxyurea analogs may undergo similar biochemical interactions across the human globin family of proteins. In fact, other heme-based enzymes, for example Catalase,[69,70] have already been identified as hydroxyurea targets. In the future, we plan to explore the binding modes and reaction kinetics of these additional redox active enzymes.

ASSOCIATED CONTENT

Supporting Information

(1) Summary of induced fit docking results of hydroxyurea analogs leading to conformation movement of residues (rmsd values) in OxyHb. (2) Summary of induced fit docking results of hydroxyurea analogs leading to conformation movement of residues (rmsd values) in MetHb. (3) ProBiS tool for binding site similarity studies. (4) ClustalW2 sequence alignment studies with human globin proteins. (5) Data for comparison of XP descriptor analysis of **6**, **6a**, and **7** obtained from IFD-XP docking in MetHb. (6) Data for analysis of second best pose that has a similar hydrogen bond with the $H_{N'}$ to any residue other than Gly25. This material is available free of charge via the Internet at http://pubs.acs.org.

AUTHOR INFORMATION

Corresponding Author

*Fax: (813) 974-3203. Tel.: (813) 974-9239. E-mail: hlw@mail.usf.edu.

Notes

The authors declare no competing financial interest.

ACKNOWLEDGMENTS

The authors would like to thank Professor Wayne Guida, Professor Randy Larsen, and Dr. Vasiliki Lykourinou for their helpful discussions. H.L.W. would like to acknowledge NIH (1K22HL088341-01A1) and the University of South Florida (start-up) for funding. Computations were performed on local USF computers and the USF Research Computing Center, where NSF-funded computational resources (under Grant No. CHE-0722887) were greatly appreciated.

ABBREVIATIONS

SCD, sickle cell disease; HbA, adult hemoglobin; HbS, sickled hemoglobin; HbF, fetal hemoglobin; NO, nitric oxide; cGMP, cyclic guanosine monophosphate; OxyHb, oxy-hemoglobin; MetHb, met-hemoglobin; DeoxyHb, deoxy-hemoglobin; HbNO, nitrosyl-hemoglobin; IFD, induced fit docking; Oxy-heme, oxygen bound to a prosthetic heme group; MetHb−HU, low-spin MetHb−hydroxyurea complex; O_{Gly25}, Gly25 carbonyl oxygen atom; HUA, hydroxyurea analog

REFERENCES

(1) Sutton, M.; Atweh, G. F.; Cashman, T. D.; Davis, W. T. Resolving conflicts: misconceptions and myths in the care of the patient with sickle cell disease. *Mt. Sinai J. Med.* **1999**, *66*, 282−285.

(2) Kotiah, S. D.; Ballas, S. K. Investigational drugs in sickle cell anemia. *Expert Opin. Invest. Drugs* **2009**, *18*, 1817−1828.

(3) Frenette, P. S.; Atweh, G. F. Sickle cell disease: old discoveries, new concepts, and future promise. *J. Clin. Invest.* **2007**, *117*, 850−858.

(4) Colombatti, R.; Maschietto, N.; Varotto, E.; Grison, A.; Grazzina, N.; Meneghello, L.; Teso, S.; Carli, M.; Milanesi, O.; Sainati, L. Pulmonary hypertension in sickle cell disease children under 10 years of age. *Br. J. Hamaetol.* **2010**, *150*, 601−609.

(5) de Franceschi, L.; Finco, G.; Vassanelli, A.; Zaia, B.; Ischia, S.; Corrocher, R. A pilot study on the efficacy of ketorolac plus tramadol infusion combined with erythrocytapheresis in the management of acute severe vaso-occlusive crises and sickle cell pain. *Haematologica* **2004**, *89*, 1389−1391.

(6) Tang, D. C.; Prauner, R.; Liu, W.; Kim, K.-H.; Hirsch, R. P.; Driscoll, M. C.; Rodgers, G. P. Polymorphisms within the

angiotensinogen gene (GT-repeat) and the risk of stroke in pediatric patients with sickle cell disease: A case-control study. *Am. J. Hematol.* **2001**, *68*, 164−169.
(7) Olowoyeye, A.; Okwundu Charles, I. Gene therapy for sickle cell disease. *Cochrane Database Syst. Rev.* **2010**, CD007652.
(8) Steinberg, M. H.; Brugnara, C. Pathophysiological-based approaches to treatment of sickle cell disease. *Annu. Rev. Med.* **2003**, *54*, 89−112.
(9) Lou, T.-F.; Singh, M.; Mackie, A.; Li, W.; Pace Betty, S. Hydroxyurea generates nitric oxide in human erythroid cells: mechanisms for gamma-globin gene activation. *Exp. Biol. Med. (Maywood)* **2009**, *234*, 1374−1382.
(10) Watson, J.; Stahman, A. W.; Bilello, F. P. The significance of the paucity of sickle cells in newborn negro infants. *Am. J. Med. Sci.* **1948**, *215*, 419−423.
(11) Noble, A., The respiratory system. In *A foundation for neonatal care: a multi-disciplinary guide*, 1 ed.; Hall, M., N., A., Smith, S., Ed.; Radcliffe Medical PR: Abingdon, Oxon, OX 1AA, U.K., 2009; pp 158−160.
(12) Charache, S.; Terrin, M. L.; Moore, R. D.; Dover, G. J.; Barton, F. B.; Eckert, S. V.; McMahon, R. P.; Bonds, D. R. Effect of hydroxyurea on the frequency of painful crises in sickle cell anemia. Investigators of the Multicenter Study of Hydroxyurea in Sickle Cell Anemia. *N. Engl. J. Med.* **1995**, *332*, 1317−1322.
(13) Weiner, D. L.; Hibberd, P. L.; Betit, P.; Copper, A. B.; Botelho, C. A.; Brugunara, C. Preliminary assessment of inhaled nitric oxide for acute vaso-occlusive crisis in pediatric patients with sickle cell disease. *JAMA, J. Am. Med. Assoc.* **2003**, *289*, 1136−1142.
(14) Cokic, V. P.; Smith, R. D.; Beleslin-Cokic, B. B.; Njoroge, J. M.; Miller, J. L.; Gladwin, M. T.; Schechter, A. N. Hydroxyurea induces fetal hemoglobin by the nitric oxide-dependent activation of soluble guanylyl cyclase. *J. Clin. Invest.* **2003**, *111*, 231−239.
(15) Singh, H.; Dulhani, N.; Kumar, B. N.; Singh, P.; Tiwari, P. Effective control of sickle cell disease with hydroxyurea therapy. *Ind. J. Pharmacol.* **2010**, *42*, 32−35.
(16) King, S. B. The nitric oxide producing reactions of hydroxyurea. *Curr. Med. Chem.* **2003**, *10*, 437−452.
(17) Huang, J.; Zou, Z.; Kim-Shapiro, D. B.; Ballas, S. K.; King, S. B. Hydroxyurea Analogues As Kinetic and Mechanistic Probes of the Nitric Oxide Producing Reactions of Hydroxyurea and Oxyhemoglobin. *J. Med. Chem.* **2003**, *46*, 3748−3753.
(18) Rohrman, B. A.; Mazziotti, D. A. Quantum Chemical Design of Hydroxyurea Derivatives for the Treatment of Sickle-Cell Anemia. *J. Phys. Chem. B* **2005**, *109*, 13392−13396.
(19) King, S. B. N-hydroxyurea and acyl nitroso compounds as nitroxyl (HNO) and nitric oxide (NO) donors. *Curr. Top. Med. Chem. (Sharjah, United Arab Emirates)* **2005**, *5*, 665−673.
(20) Lepeshkevich, S. V.; Parkhats, M. V.; Stepuro, I. I.; Dzhagarov, B. M. Molecular oxygen binding with α and β subunits within the R quaternary state of human hemoglobin in solutions and porous sol-gel matrices. *Biochim. Biophys. Acta, Proteins Proteomics* **2009**, *1794*, 1823−1830.
(21) Safo, M. K.; Ahmed, M. H.; Ghatge, M. S.; Boyiri, T. Hemoglobin-ligand binding: Understanding Hb function and allostery on atomic level. *Biochim. Biophys. Acta, Proteins Proteomics* **2011**, *1814*, 797−809.
(22) Park, S.-Y.; Yokoyama, T.; Shibayama, N.; Shiro, Y.; Tame, J. R. H. 1.25 Å resolution crystal structures of human hemoglobin in the oxy, deoxy and carbonmonoxy forms. *J. Mol. Biol.* **2006**, *360*, 690−701.
(23) Yuan, Y.; Simplaceanu, V.; Ho, N. T.; Ho, C. An Investigation of the Distal Histidyl Hydrogen Bonds in Oxyhemoglobin: Effects of Temperature, pH, and Inositol Hexaphosphate. *Biochemistry* **2010**, *49*, 10606−10615.
(24) Kanias, T.; Acker, J. P. Biopreservation of red blood cells - the struggle with hemoglobin oxidation. *Febs J.* **2010**, *277*, 343−356.
(25) Bellelli, A. Hemoglobin and cooperativity: experiments and theories. *Curr. Protein Pept. Sci.* **2010**, *11*, 2−36.
(26) Yonetani, T.; Laberge, M. Protein dynamics explain the allosteric behaviors of hemoglobin. *Biochim. Biophys. Acta, Proteins Proteomics* **2008**, *1784*, 1146−1158.
(27) Dzhagarov, B. M.; Lepeshkevich, S. V. Kinetic studies of differences between α- and β-chains of human hemoglobin: an approach for determination of the chain affinity to oxygen. *Chem. Phys. Lett.* **2004**, *390*, 59−64.
(28) Umbreit, J. Methemoglobin-it's not just blue: a concise review. *Am. J. Hematol.* **2007**, *82*, 134−144.
(29) King, S. B. C-Nitroso compounds, oximes, N-hydroxyguanidines and N-hydroxyureas. *Nitric Oxide Donors* **2005**, 177−199.
(30) Huang, J.; Hadimani, S. B.; Rupon, J. W.; Ballas, S. K.; Kim-Shapiro, D. B.; King, S. B. Iron Nitrosyl Hemoglobin Formation from the Reactions of Hemoglobin and Hydroxyurea. *Biochemistry* **2002**, *41*, 2466−2474.
(31) Pacelli, R.; Taira, J.; Cook, J. A.; Wink, D. A.; Krishna, M. C. Hydroxyurea reacts with heme proteins to generate nitric oxide. *Lancet* **1996**, *347*, 900.
(32) Sherman, W.; Beard, H. S.; Farid, R. Use of an induced fit receptor structure in virtual screening. *Chem. Biol. Drug Des.* **2006**, *67*, 83−84.
(33) Sherman, W.; Day, T.; Jacobson, M. P.; Friesner, R. A.; Farid, R. Novel Procedure for Modeling Ligand/Receptor Induced Fit Effects. *J. Med. Chem.* **2006**, *49*, 534−553.
(34) Konc, J.; Cesnik, T.; Konc, J. T.; Penca, M.; Janezic, D. ProBiS-Database: Precalculated Binding Site Similarities and Local Pairwise Alignments of PDB Structures. *J. Chem. Inf. Model.* **2012**, *52*, 604−612.
(35) Konc, J.; Janezic, D. ProBiS algorithm for detection of structurally similar protein binding sites by local structural alignment. *Bioinformatics* **2010**, *26*, 1160−1168.
(36) Konc, J.; Janezic, D. ProBiS: a web server for detection of structurally similar protein binding sites. *Nucleic Acids Res.* **2010**, *38*, W436−W440.
(37) Larkin, M. A.; Blackshields, G.; Brown, N. P.; Chenna, R.; McGettigan, P. A.; McWilliam, H.; Valentin, F.; Wallace, I. M.; Wilm, A.; Lopez, R.; Thompson, J. D.; Gibson, T. J.; Higgins, D. G. Clustal W and Clustal X version 2.0. *Bioinformatics* **2007**, *23*, 2947−2948.
(38) Chen, H.; Ikeda-Saito, M.; Shaik, S. Nature of the Fe-O2 Bonding in Oxy-Myoglobin: Effect of the Protein. *J. Am. Chem. Soc.* **2008**, *130*, 14778−14790.
(39) Park, S.-Y.; Yokoyama, T.; Shibayama, N.; Shiro, Y.; Tame Jeremy, R. H. 1.25 A resolution crystal structures of human haemoglobin in the oxy, deoxy and carbonmonoxy forms. *J. Mol. Biol.* **2006**, *360*, 690−701.
(40) Dodson, E.; Dodson, G. Movements at the hemoglobin A-hemes and their role in ligand binding, analyzed by X-ray crystallography. *Biopolymers* **2009**, *91*, 1056−1063.
(41) De Rosa, M. C.; Alinovi, C. C.; Russo, A.; Giardina, B. Binding modes of L35 to α- and β-semihemoglobins: Structural insights into the inequivalence of α- and β-subunits of hemoglobin. *Biochem. Biophys. Res. Commun.* **2007**, *354*, 720−726.
(42) Marechal, J.-D.; Maseras, F.; Lledos, A.; Mouawad, L.; Perahia, D. A DFT study on the relative affinity for oxygen of the α and β subunits of hemoglobin. *J. Comput. Chem.* **2006**, *27*, 1446−1453.
(43) Birukou, I.; Schweers, R. L.; Olson, J. S. Distal Histidine Stabilizes Bound O2 and Acts as a Gate for Ligand Entry in Both Subunits of Adult Human Hemoglobin. *J. Biol. Chem.* **2010**, *285*, 8840−8854.
(44) Lukin, J. A.; Simplaceanu, V.; Zou, M.; Ho, N. T.; Ho, C. NMR reveals hydrogen bonds between oxygen and distal histidines in oxyhemoglobin. *Proc. Natl. Acad. Sci. U.S.A.* **2000**, *97*, 10354−10358.
(45) Suzuki, T.; Watanabe, Y.-H.; Nagasawa, M.; Matsuoka, A.; Shikama, K. Dual nature of the distal histidine residue in the autoxidation reaction of myoglobin and hemoglobin. Comparison of the H64 mutants. *Eur. J. Biochem.* **2000**, *267*, 6166−6174.
(46) Friesner, R. A.; Murphy, R. B.; Repasky, M. P.; Frye, L. L.; Greenwood, J. R.; Halgren, T. A.; Sanschagrin, P. C.; Mainz, D. T. Extra Precision Glide: Docking and Scoring Incorporating a Model of

Hydrophobic Enclosure for Protein-Ligand Complexes. *J. Med. Chem.* **2006**, *49*, 6177−6196.
(47) Jacobson, M. P.; Friesner, R. A.; Xiang, Z.; Honig, B. On the Role of the Crystal Environment in Determining Protein Side-chain Conformations. *J. Mol. Biol.* **2002**, *320*, 597−608.
(48) Jacobson, M. P.; Pincus, D. L.; Rapp, C. S.; Day, T. J. F.; Honig, B.; Shaw, D. E.; Friesner, R. A. A hierarchical approach to all-atom protein loop prediction. *Proteins Struct., Funct., Bioinf.* **2004**, *55*, 351−367.
(49) Agostino, M.; Jene, C.; Boyle, T.; Ramsland, P. A.; Yuriev, E. Molecular Docking of Carbohydrate Ligands to Antibodies: Structural Validation against Crystal Structures. *J. Chem. Inf. Model.* **2009**, *49*, 2749−2760.
(50) Jorgensen, W. L.; Maxwell, D. S.; Tirado-Rives, J. Development and Testing of the OPLS All-Atom Force Field on Conformational Energetics and Properties of Organic Liquids. *J. Am. Chem. Soc.* **1996**, *118*, 11225−11236.
(51) Vanommeslaeghe, K.; Hatcher, E.; Acharya, C.; Kundu, S.; Zhong, S.; Shim, J.; Darian, E.; Guvench, O.; Lopes, P.; Vorobyov, I.; Mackerell, A. D., Jr. CHARMM general force field: A force field for drug-like molecules compatible with the CHARMM all-atom additive biological force fields. *J. Comput. Chem.* **2010**, *31*, 671−690.
(52) Wang, J.; Wolf, R. M.; Caldwell, J. W.; Kollman, P. A.; Case, D. A. Development and testing of a general Amber force field. *J. Comput. Chem.* **2004**, *25*, 1157−1174.
(53) Kolossvary, I.; Guida, W. C. Low-mode conformational search elucidated: application to C39H80 and flexible docking of 9-deazaguanine inhibitors into PNP. *J. Comput. Chem.* **1999**, *20*, 1671−1684.
(54) Gadakar, P. K.; Phukan, S.; Dattatreya, P.; Balaji, V. N. Pose Prediction Accuracy in Docking Studies and Enrichment of Actives in the Active Site of GSK-3β. *J. Chem. Inf. Model.* **2007**, *47*, 1446−1459.
(55) Celik, L.; Sinning, S.; Severinsen, K.; Hansen, C. G.; Moller, M. S.; Bols, M.; Wiborg, O.; Schiott, B. Binding of Serotonin to the Human Serotonin Transporter. Molecular Modeling and Experimental Validation. *J. Am. Chem. Soc.* **2008**, *130*, 3853−3865.
(56) Liao, C.; Park, J.-E.; Bang, J. K.; Nicklaus, M. C.; Lee, K. S. Probing Binding Modes of Small Molecule Inhibitors to the Polo-Box Domain of Human Polo-like Kinase 1. *ACS Med. Chem. Lett.* **2010**, *1*, 110−114.
(57) Felts, A. K.; LaBarge, K.; Bauman, J. D.; Patel, D. V.; Himmel, D. M.; Arnold, E.; Parniak, M. A.; Levy, R. M. Identification of Alternative Binding Sites for Inhibitors of HIV-1 Ribonuclease H Through Comparative Analysis of Virtual Enrichment Studies. *J. Chem. Inf. Model.* **2011**, *51*, 1986−1998.
(58) Babaoglu, K.; Shoichet, B. K. Deconstructing fragment-based inhibitor discovery. *Nat. Chem. Biol.* **2006**, *2*, 720−723.
(59) McRobb, F. M.; Capuano, B.; Crosby, I. T.; Chalmers, D. K.; Yuriev, E. Homology Modeling and Docking Evaluation of Aminergic G Protein-Coupled Receptors. *J. Chem. Inf. Model.* **2010**, *50*, 626−637.
(60) Barreca, M. L.; Iraci, N.; De Luca, L.; Chimirri, A. Induced-Fit Docking Approach Provides Insight into the Binding Mode and Mechanism of Action of HIV-1 Integrase Inhibitors. *ChemMedChem* **2009**, *4*, 1446−1456.
(61) Brooks, B. R.; Bruccoleri, R. E.; Olafson, B. D.; States, D. J.; Swaminathan, S.; Karplus, M. CHARMM: a program for macromolecular energy, minimization, and dynamics calculations. *J. Comput. Chem.* **1983**, *4*, 187−217.
(62) Miller, B. T.; Singh, R. P.; Klauda, J. B.; Hodoscek, M.; Brooks, B. R.; Woodcock, H. L., III CHARMMing: A New, Flexible Web Portal for CHARMM. *J. Chem. Inf. Model.* **2008**, *48*, 1920−1929.
(63) Brooks, B. R.; Brooks, C. L., III; Mackerell, A. D., Jr.; Nilsson, L.; Petrella, R. J.; Roux, B.; Won, Y.; Archontis, G.; Bartels, C.; Boresch, S.; Caflisch, A.; Caves, L.; Cui, Q.; Dinner, A. R.; Feig, M.; Fischer, S.; Gao, J.; Hodoscek, M.; Im, W.; Kuczera, K.; Lazaridis, T.; Ma, J.; Ovchinnikov, V.; Paci, E.; Pastor, R. W.; Post, C. B.; Pu, J. Z.; Schaefer, M.; Tidor, B.; Venable, R. M.; Woodcock, H. L.; Wu, X.; Yang, W.; York, D. M.; Karplus, M. CHARMM: The biomolecular simulation program. *J. Comput. Chem.* **2009**, *30*, 1545−1614.
(64) Misra, H. P.; Fridovich, I. Generation of superoxide radical during the autoxidation of hemoglobin. *J. Biol. Chem.* **1972**, *247*, 6960−6962.
(65) Konc, J. J., D. An Improved Branch and Bound Algorithm for the Maximum Clique Problem MATCH Commun. *Math. Comput. Chem.* **2007**, *58*, 569−590.
(66) Simonneaux, G.; Bondon, A. Mechanism of electron transfer in heme proteins and models: The NMR approach. *Chem. Rev.* **2005**, *105*, 2627−2646.
(67) Kiger, L.; Marden, M. C. Electron transfer kinetics between hemoglobin subunits. *J. Biol. Chem.* **2001**, *276*, 47937−47943.
(68) Li, C.-z.; Liu, G.; Prabhulkar, S. Comparison of kinetics of hemoglobin electron transfer in solution and immobilized on electrode surface. *Am. J. Biomed. Sci.* **2009**, *1*, 283−294.
(69) Huang, J.; Kim-Shapiro, D. B.; King, S. B. Catalase-Mediated Nitric Oxide Formation from Hydroxyurea. *J. Med. Chem.* **2004**, *47*, 3495−3501.
(70) Juul, T.; Malolepszy, A.; Dybkaer, K.; Kidmose, R.; Rasmussen, J. T.; Andersen, G. R.; Johnsen, H. E.; Jorgensen, J.-E.; Andersen, S. U. The in Vivo Toxicity of Hydroxyurea Depends on Its Direct Target Catalase. *J. Biol. Chem.* **2010**, *285*, 21411−21415.